Czech Technical University in Prague
Faculty of Electrical Engineering
Department of Control Engineering

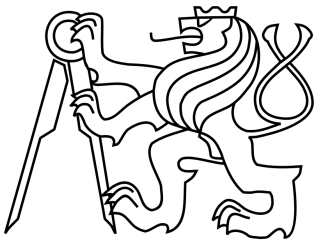

Bachelor Thesis

Modelling of dielectrophoresis for feedback control

Author: Ivan Nikolaev

Tutor: Ing. Jiří Zemánek

Prague, 2012

Acknowledgment

I would like to thank Jiří Zemánek for being a helpful and knowledgable tutor without whose guidance I would not be able to complete this work. I would also like to thank my mother who has always given me her full support.

Declaration

I declare that I have created this bachelor thesis by myself and have only used the sources provided in the list of references.

Prague ....

Signature

Abstract

This work deals with simulation of behaviour of microscopic particles subjected to dielectrophoretic forces. The goal is to create a simulation which will help to design and test a feedback control algorithm.

In this work a hybrid approach to simulation is taken which consists of two parts: preprocessing and simulation. Preprocessing is done in Comsol Multiphysics. The data from preprocessing is then used for the simulation which is done in Matlab. Preprocessing helps to speed up the simulation by avoiding unnecessary repetition of the same calculations.

The simulation is then compared with numerical and analytical solutions as well as laborarotary experiments.

Abstrakt

V této práci budeme simulovat chování mikroskopických částic pod vlivem dielektroforetické síly. Našim cílem je vytvořit simulaci, kterou bude možné použít při návrhu zpětnovazebního řízení. Při tvorbě simulace aplikujeme hybridní přístup, který se skládá ze dvou částí: přípravný výpočet (předvýpočet) a samotná simulace. Přípravný výpočet (předvýpočet) provedeme v programu Comsol Mutyphisycs, který nám umožní simulaci urychlit omezením opakování stejných výpočtů. Získaná data pak použijeme při simulaci, kterou provedeme v Matlabu. Simulaci následně porovnáme s numerickými a analytickými řešeními a také s laboratorními experimenty.

Contents

1 Introduction

The goal of this work is to create a simulation of the behaviour of particles subjected to dielectrophoretic force. The simulation can then be used to help analyse the behaviour of particles under different electrode configurations, frequencies and voltage patterns. The simulation can also be used to create an MPC controller, which requires a model for its operation.

In the first part the theory behind dielectrophoresis is presented. In the second part different simulation approaches are explained. In the third part the author's simulations are presented. In the fourth the results of the simulations are compared with each other and with experimental results.

2 Dielectrophoresis

Dielectrophoresis is a phenomenon that describes a force experienced by polarizable particles when subjected to non-uniform electric field. The particles are generally in the 1 to 1000 µm range. For bigger particles the effects of gravity usually prevail and for smaller particles the behaviour of individual particles becomes upredictable due to effects of Brownian motion. The field can be either DC or AC. In AC fields the forces depend on the frequency and different frequencies result in different phenomena like positive and negative dielectrophoresis or travelling wave dielectrophoresis. In this section the theory behind dielectrophoresis is briefly explained for the benefit of the reader and for easy referencing from later sections. The theory is taken from [1] and [2]

2.1 Dielectrophoretic force

Dielectrophoresis occurs when a polarizable particle is exposed to an electric field. The electric field causes a dipole to form within the material. If the field is uniform, the forces on the dipole charges are equal and act in opposite directions, so that the net force is zero. In a non-uniform field however the force on one charge will be different from the force on the other charge resulting in a net force on the particle. The force is referred to as the dielectroforetic force and the phenomena is known as dielectrophoresis.

If we consider a dipole with charges separated by vector $\mathbf{d}$ at location $\mathbf{r}$, then the net force on the particle can be described by the Equation (2.1)

$$\mathbf{F} = Q^{+}\mathbf{E}(\mathbf{r}+\mathbf{d}) - Q^{-}\mathbf{E}(\mathbf{r}) \tag{2.1}$$

Since $\mathbf{d}$ is small relative to the size of the field non-uniformity, we can make an approximation

$$\mathbf{E}(\mathbf{r}+\mathbf{d}) = \mathbf{E}(\mathbf{r}) + \mathbf{d}\cdot\nabla\mathbf{E}(\mathbf{r}) \tag{2.2}$$

and rewrite the force as:

$$\mathbf{F} = Q\mathbf{d} \cdot \nabla \mathbf{E} \tag{2.3}$$

The dipole moment is defined as:

$$\mathbf{m} = Q\mathbf{d} \tag{2.4}$$

Therefore we can rewrite the force equation as:

$$\mathbf{F} = (\mathbf{m} \cdot \nabla)\mathbf{E} \tag{2.5}$$

For spherical dielectric particles the dipole moment is described by the following equation:

$$\mathbf{m}(\omega) = 4\pi R^3 \epsilon_0 K(\omega)\mathbf{E} \tag{2.6}$$

where R is the radius of the sphere, ϵ_0 is the permittivity of vacuum and $K(\omega)$ is the Clausius-Mossotti factor, dependent on the frequency.

If we consider $\mathbf{E}$ as a phasor $\tilde{\mathbf{E}}$, then $\mathbf{m}(\omega)$ also becomes a phasor and the time-averaged force can be given by

$$\mathbf{F} = \frac{1}{2} Re[(\tilde{\mathbf{m}}(\omega) \cdot \nabla)\tilde{\mathbf{E}}^*] \tag{2.7}$$

By substituting the dipole moment phasor we can rewrite the expression as

$$8\pi R^3 \epsilon_0 K(\omega)(\tilde{\mathbf{E}} \cdot \nabla)\tilde{\mathbf{E}}^* = 4\pi R^3 \epsilon_0 K(\omega)(\tilde{\mathbf{E}} \cdot \tilde{\mathbf{E}}^*) - 4\pi R^3 \epsilon_0 K(\omega)\nabla \times (\tilde{\mathbf{E}} \times \tilde{\mathbf{E}}^*) \tag{2.8}$$

. This uses two identities:

$$\nabla(\mathbf{A} \cdot \mathbf{B}) = (\mathbf{B} \cdot \nabla)\mathbf{A} + (\mathbf{A} \cdot \nabla)\mathbf{B} + \mathbf{B} \times (\nabla \times \mathbf{A}) + \mathbf{A} \times (\nabla \times \mathbf{B}) \tag{2.9}$$

and

$$\nabla \times (\mathbf{A} \times \mathbf{B}) = (\mathbf{B} \cdot \nabla)\mathbf{A} - (\mathbf{A} \cdot \nabla)\mathbf{B} + (\nabla \cdot \mathbf{B})\mathbf{A} - (\nabla \cdot \mathbf{A})\mathbf{B} \tag{2.10}$$

and the fact that the electric field is irrotational, i.e. $\nabla \times \tilde{\mathbf{E}} = 0$ and Gauss's law with zero free charge density, i.e. $\nabla \cdot \tilde{\mathbf{E}} = 0$. The time-averaged force then becomes:

$$\mathbf{F}_{DEP} = \pi R^3 \epsilon_0 \epsilon_m Re[K(\omega)] \nabla (|Re[\tilde{\mathbf{E}}]|^2 + |Im[\tilde{\mathbf{E}}]|^2) \tag{2.11}$$

$$\mathbf{F}_{twDEP} = -2\pi R^3 \epsilon_0 \epsilon_m Im[K(\omega)] (\nabla \times Re[\tilde{\mathbf{E}}] \times Im[\tilde{\mathbf{E}}]) \tag{2.12}$$

Equation (2.11) gives time-averaged force for conventional dielectrophoresis. Equation (2.12) gives time-averaged force for travelling wave dielectrophoresis.

2.2 Clausius-Mossotti factor

The dielectrophoretic force is frequency-dependent. The frequency dependance is given by the Clausius-Mossotti factor which is defined in the following equation:

$$K(\omega) = \frac{\epsilon_p^* - \epsilon_m^*}{\epsilon_p^* + 2\epsilon_m^*} \tag{2.13}$$

where ϵ_m^* and ϵ_p^* are the complex permittivity of the medium and particle and $\epsilon^* = \epsilon - j(\sigma/\omega)$, where ϵ is the permittivity, σ is the conductivity and ω is the angular frequency. The real part of the Clausius-Mossotti factor determines the dielecrophoretic force the imaginary part determines the travelling wave dielctrophoretic force. Clausius-Mossotti factor is shown in Figure 2.1 for $\epsilon_m = 78$, $\sigma_m = 0.001$, $\epsilon_p = 2.55$ and $\sigma_p = 0.01$(water and polystyrene). It can be seen that for frequencies below approximately 1.76 MHz the real part is positive and for the frequencies above that the real part is negative.

The frequency where $Re[K(\omega)] = 0$ is called the cross-over frequency. At that frequency dielectrophoretic force does not act on the particles and the travelling wave dielctrophoresis becomes most prominent. For frequencies below the cross-over frequency the force experienced by the particles is towards the electrodes. It is called positive dielectrophoresis. For frequencies above the cross-over frequency the force is in the opposite direction, away from the electrode, which is referred to as negative dielectrophoresis.

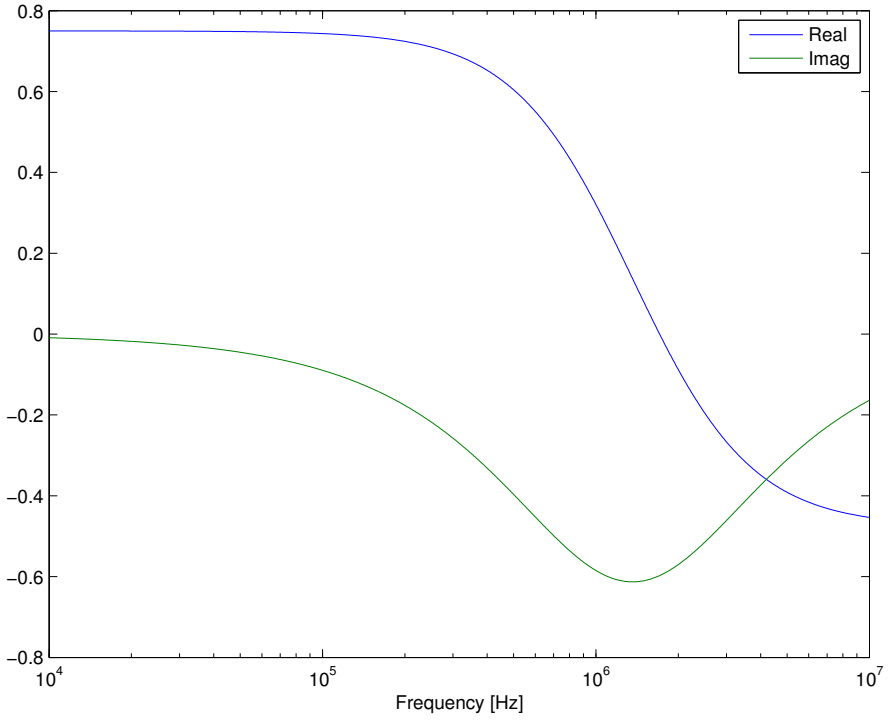

Figure 2.1: Clausius-Mossotti factor for polystyrene in deionised water.

2.3 Actuators

There are many possible electrode actuator combinations used for creating electric fields. In this work we will be considering a simple parallel electrode

array while taking into consideration potential future extension for more complex configurations.

2.4 Other forces

Other forces which are not dielectrophoretic but are nevertheless important in simulating the motion of a particle subjected to dielectrophoresis are: viscous drag, buoyancy and brownian motion.

2.4.1 Viscous drag

Viscous drag is a friction force that retards the motion of a particle moving through a fluid. The viscous drag force is very significant for colloidal particles, so that they reach their terminal velocity in a few nanoseconds. For a spherical particle of radius r the terminal velocity can be determined by Stoke's law and is given by the expression:

$$\mathbf{F} = -6\pi\eta r\mathbf{V} \tag{2.14}$$

where η is the viscosity of the medium.

2.4.2 Buoyancy

The particles also experience the force of gravity. The force is usually very small, but can be observed over time. The force is given by the equation:

$$\mathbf{F}_{sediment} = \nu(\rho_m - \rho_p)\mathbf{g} \tag{2.15}$$

where ν is the volume of the particle, ρ_m and ρ_p are the densities of the medium and the particle. If the particle is denser than the medium it will sink(sediment) over time if it is less dense than the medium it will float.

2.4.3 Brownian motion

All the particles are subject to Brownian motion. The effect is more pronounced for smaller particles. For bigger particles random collision tend to cancel each other out more evenly. The mean displacement due to Brownian motion for spherical particles is given by

$$|\triangle d| = \sqrt{\frac{k_B T t}{3\pi\eta r}} \tag{2.16}$$

where k_B is the Boltzmann constant, T is the temparture in Kelvin, r is the radius of the particle and η is the viscosity of the medium.

Brownian motion is important because although the time-averaged force is zero the mean displacement is non-zero which means it has to be overcome by the dielectrophoretic force in order to successfully control the particle.

3 Simulation approaches

There are different simulation approaches for dielectrophoresis. In this part we are going to look at some of them and discuss their advantages and disadvantages. We will be looking at analytical, numerical and hybrid approaches.

3.1 Analytical

The analytical approach to simulation attempts to find the dielectrophoretic forces by deriving the equations that give the dielectrophoretic force for specific electrode configurations. Analytical simulations give fast and precise results. However, analytical solutions are hard to find even for the simple electrode arrays. They become nearly impossible for more complex electrode arrays which makes them impractical for real-life applications.

In this paper we implement a simulation from [3] for two-phase electrode array with approximate boundary condition, as well as two-phase electrode array with exact boundary condition. Approximate boundary condition assumes that the the potential at y=0 between the electrodes changes linearly. The exact boundary condition assumes that the normal derivative of the potential is zero at the boundary between the electrodes. The simulations are done by simply solving an equation at specified coordinates and electrode ratio parameters. d_1 being the width of the electrode, d_2 the gap between the electrodes, V the applied voltage and x and y the coordinates. $G(\omega)$ is the product of Clausius-Mossotti factor and the volume of the particle.

The equation for the approximate boundary condition two-phase electrode is:

$$\mathbf{F}_{DEP} = \frac{16V^2}{\pi d(d_2)^2} Re[G(\omega)] \cdot Re \begin{bmatrix} izh(\bar{z}; \frac{d_1}{4d})h'(z; \frac{d_1}{4d}) \\ -zh(\bar{z}; \frac{d_1}{4d})h'(z; \frac{d_1}{4d}) \end{bmatrix} \tag{3.1}$$

where $d = (d_1 + d_2)/2$, $z = exp(\frac{\pi(ixy}{2d})$, $\bar{z} = exp(\frac{-\pi(ix+y)}{2d})$, $h(z;q) = \frac{1}{4}ln(\frac{1+2zcos(q\pi)+z^2}{1-2zcos(q\pi)+z^2})$, $h'(z;q) = \frac{(1-z^2)cos(q\pi)}{1-2z^2cos(2q\pi)+z^4}$.

The equation for the exact boundary condition two-phase electrode is:

$$\mathbf{F}_{DEP} = \frac{\pi^3 V^2}{2K^2(cos(\pi q/2))d^3} Re[G(\omega)] \cdot Re \begin{bmatrix} izk(\bar{z};q)k'(z;q) \\ -zk(\bar{z};q)k'(z;q) \end{bmatrix} \tag{3.2}$$

where $d = (d_1 + d_2)/2$, $q = d_1/(2d)$, $z = exp(\frac{\pi(ix-y)}{d})$, $\bar{z} = exp(-\frac{\pi(ix+y)}{d})$, $k(z;q) = (\frac{z}{1-2zcos(q\pi)+z^2})^{1/2}$, $k'(z;q) = \frac{1-z^2}{2k(z;q)(1-2zcos(q\pi)+z^2)^2}$ and K is the complete elliptic function of the first kind.

3.2 Numerical

Numerical simulations are based on finite element method software. The simulation for parallel electrode array can be done in 2d since the length of the electrodes is significantly greater than their width. They can also assumed to be infinitely thin, since their width is significantly greater than their thickness. The resulting solution will be incorrect close to the electrode edges, but that is not so important since the DEP force approximation is invalid in that region anyway due to rapid variations of the electric field[2].

It is important to define proper boundary conditions for the FEM software, otherwise the results will be highly distorted. There are two boundary conditions that can be used: the Neumann boundary condition for the electric potential in the electrolyte ($\partial\tilde{\phi}/\partial n = 0$, where $\mathbf{n}$ is the normal to the boundary and $\tilde{\phi}$ is the electric potential phasor). The other condition is the Dirichlet condition ($\tilde{\phi} = 0$). The lower boundary must be assigned the Neumann boundary condition, due to current conservation argument. The upper boundary condition can be either Neumann or Dirichlet. It should be placed high above the area of interest to make sure it does not influence the results.

The side conditions can be determined through a symmetry argument for symmetrical electrode arrangements and specific potentials. Consider an electrode array shown in Figure 3.1. The electrodes have 90 ° phase shift between them. We have chosen to simulate the area between 0 ° and 90 °

electrodes. The boundaries cut the electrodes in half, we can use the Dirichlet boundary condition for the boundary above the electrodes whose elecric potential is 0, because they are located midway between two electrodes with equal electric potential of opposite signs. Boundary going through the electrodes with non-zero electric potential should be assigned the Neumann condition as it is the symmetry axis between two 0 electric potentials.

Numerical simulations theory is taken from [2]

3.3 Hybrid

Hybrid simulation uses the power of numerical simulation for preprocessing data for different array configurations and then using the preprocessed data to quickly find the force when it's required. In this work we will use the approach from [4].

This approach uses bidimensional electrode meshing principle for preprocessing. The electrodes are all meshed along directions x and y. Figure 3.2 shows an example of mesh for a 4 electrode parallel array. A voltage is applied to one electrode while the rest are kept at zero. The surface charge on the electrodes is then calculated and integrated on each mesh piece. Each mesh piece is then represented by an elementary charge located at its center. The process is done for n electrodes for an (n+1)-electrode matrix. One electrode is always kept at zero and is used as the reference one. The electric field is the sum of contributions of elementary charges $Q_{r,s}$ at point $P(r,s)$. The electric field is then:

$$\mathbf{E}(x,y,z) = \frac{1}{2\pi\epsilon_0\epsilon_m}\sum_{r=1}^{e_x}\sum_{s=1}^{e_y} Q_{r,s}\cdot\frac{\overrightarrow{P(r,s)M(x,y,z)}}{||\overrightarrow{P(r,s)M(x,y,z)}||^3}ds \tag{3.3}$$

$Q_{r,s}$ can be calculated using the superposition principle:

$$Q_{r,s} = \sum_{m=1}^{n} C_{r,s,m}\cdot U_m \tag{3.4}$$

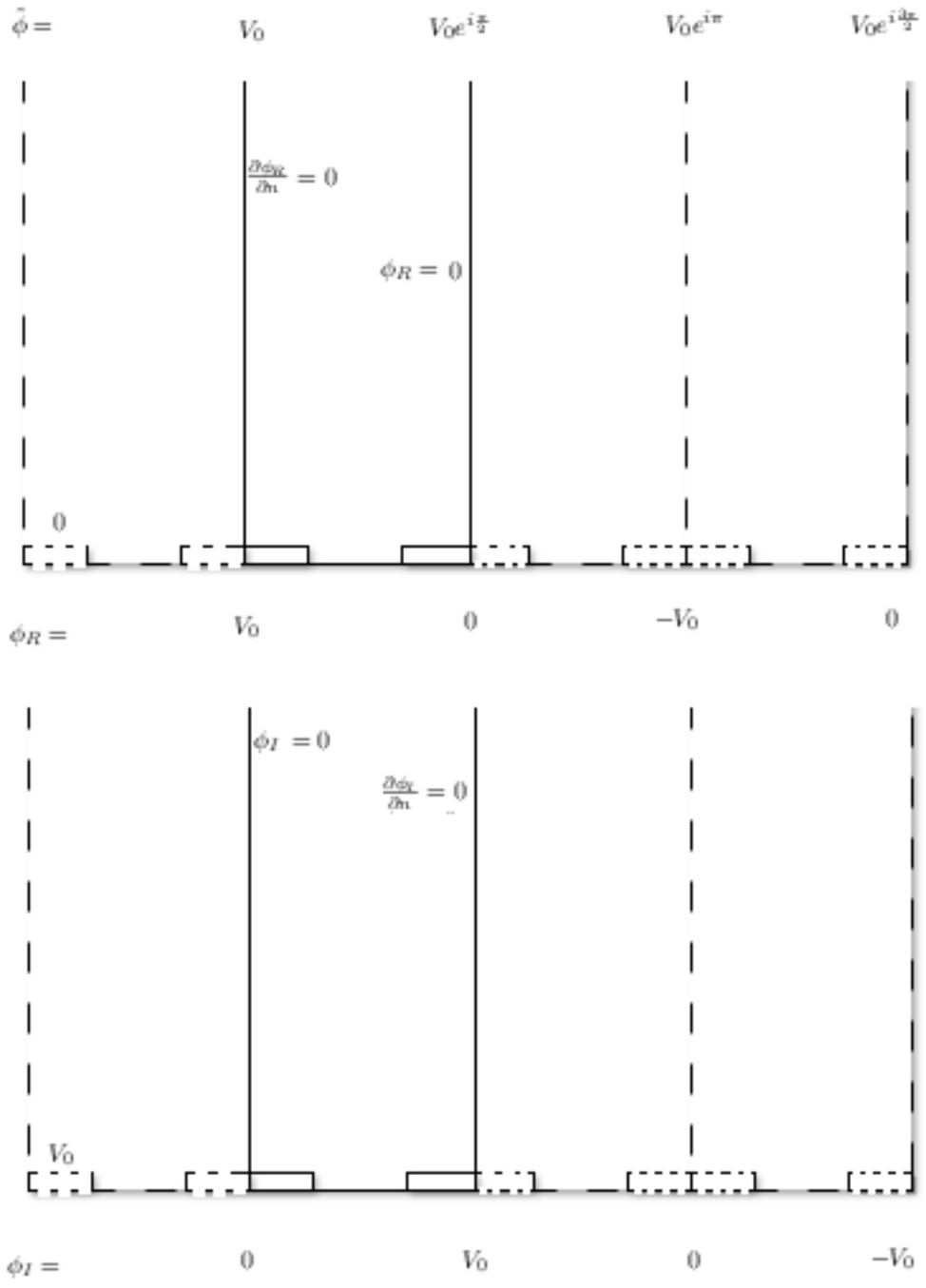

Figure 3.1: 2d boundary conditions. $\tilde{\phi}$ represents the electric potential phasor. $\phi_R = Re[\tilde{\phi}]$ and $\phi_I = Im[\tilde{\phi}]$. Redrawn from [3].

$$U = [U_1 = \vartheta_1 - \vartheta_0, ..., U_n = \vartheta_n - \vartheta_0] \tag{3.5}$$

The preprocessed data consists of the capacitance matrix $C_{r,s,m}$ of size (number of mesh elements in x direction, number of mesh elements in y direction, number of electrodes − 1). Once $\mathbf{E}$ is known, the force can be calculated using Equations (2.11) and (2.12).

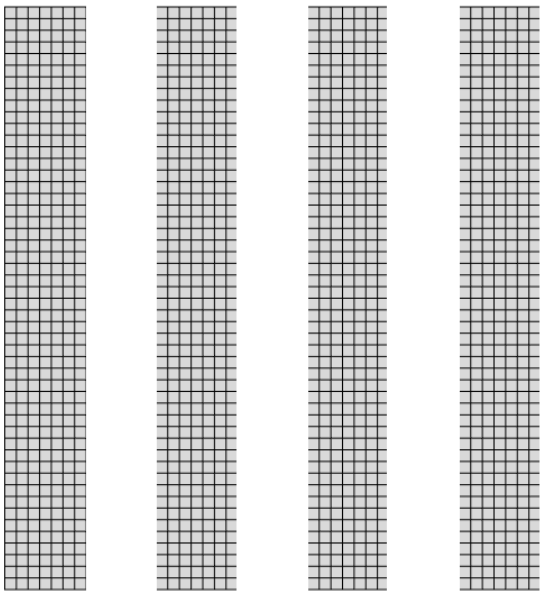

Figure 3.2: Hybrid electrode meshing. Parallel electrode array.

3.4 Dynamic trajectory modeling

In order to simulate the trajectory of a particle subjected to dielectrophoretic force a dynamic type of simulation is required. Approach from [4] is explained below.

Using the Newton's second law, the motion of the particle is defined by

the following equation:

$$\mathbf{F}_{DEP} + \mathbf{F}_{sediment} + \mathbf{F}_{drag} = m\mathbf{a} \tag{3.6}$$

Where $\mathbf{F}_{DEP}$ is the dielectrophoretic force described by Equations (2.11) and (2.12). $\mathbf{F}_{sediment}$ is the buyoancy force defined in Equation (2.15), $\mathbf{F}_{drag}$ is the drag force defined in Equation (2.14), m is the mass of the particle and $\mathbf{a}$ is the acceleration of the particle. Because the m constant is so small, the $m\mathbf{a}$ term can be neglected. The equation can then be rewritten as:

$$\mathbf{V} = \frac{\mathbf{F}_{DEP} + \mathbf{F}_{\mathbf{sediment}}}{6\pi\eta r} \tag{3.7}$$

Since the terminal velocity is reached in such a short time, the particle can be considered to be always moving at its terminal velocity, which means that Equation (3.7) expresses the velocity of the particle given the forces on it.

3.5 Surface charge density

For the hybrid simulation it is important to be able to calculate the surface charge density on the electrodes. We shall examine two approaches.

3.5.1 Finite element analysis

It is possible to use FEM software like Comsol multiphysics and then extract the surface charge density data from it.

3.5.2 The method of moments

Another way to calculate the surface charge density is by using the method of moments. The method of moments divides the surface into a series of singular charges whose contributions to the electric field are determined by the Coulomb's law. Given known electrical potential and distance between

the charges, it is possible to determine the value of each charge and hence approximate the surface charge density.

If we approximate the system of electrodes as n electrode subareas each one with known potential V then we can describe the potential on each electrode in terms of the potential on itself and on all the other charges:

$$V_1 = p_{11}q_1 + p_{12}q_2 + ... + p_{1n}q_n$$

$$V_2 = p_{21}q_1 + p_{22}q_2 + ... + p_{2n}q_n$$

$$V_3 = p_{31}q_1 + p_{32}q_2 + ... + p_{3n}q_n \tag{3.8}$$

$$.$$

$$V_n = p_{n1}q_1 + p_{n2}q_2 + ... + p_{nn}q_n$$

p_{ij} is the potential on subarea i from a unit charge on potential j in the absence of any other charges. V_i is the potential on subarea i, q_i is the charge on subarea i.

$$p_{ij} = \frac{1}{4\pi\epsilon_0\epsilon_m}\int \frac{\sigma_j|dA_j|}{|r_{ij}|} \tag{3.9}$$

Where ϵ_m is the relative permittivity of the medium, σ_j is the surface charge density on subarea j. Since j holds unit charge $\sigma_j = \frac{1}{A_j}$. r_{ij} is the distance between the charges. The above integration is given by, provided the rectangle j does not cross the x or y axes

$$4\pi\epsilon_0\epsilon_m A_j p_{ij} = |I(x_2, y_2) - I(x_2, y_1) - I(x_1, y_2) + I(x_1, y_1)| \tag{3.10}$$

where

$$I = x \cdot sinh^{-1}(\frac{y}{|x|}) + y \cdot sinh^{-1}(\frac{x}{|y|}) \tag{3.11}$$

If the rectangle crosses the x or y axes, it should be subdivided into two(or four) rectangles that do not cross the axes. Expression 3.8 can be written in vector form:

$$\begin{pmatrix} V_1 \\ V_2 \\ . \\ V_n \end{pmatrix} = \begin{pmatrix} p_{11} & p_{12} & . & p_{1n} \\ p_{21} & p_{22} & . & p_{2n} \\ . & . & . & . \\ p_{n1} & p_{n2} & . & p_{nn} \end{pmatrix} \begin{pmatrix} q_1 \\ q_2 \\ . \\ q_n \end{pmatrix} \tag{3.12}$$

Or:

$$\mathbf{V} = \mathbf{PQ} \tag{3.13}$$

The charge $\mathbf{Q}$ can therefore be found as:

$$\mathbf{Q} = \mathbf{P}^{-1}\mathbf{V} \tag{3.14}$$

The method of moments theory is taken from [1].

4 Simulations

In this section the author's simulations are presented. During the making of these simulations the author encountered many problems and dead ends. Some of these will be presented here in order to show the amount of work done as well as warn anyone who reads this of the complications they may encounter shall they attempt to create a similar simulation.

Simulations show $\nabla \mathbf{E}^2$ for the dielectrophoretic force and $\nabla \times Re[\tilde{\mathbf{E}}] \times Im[\tilde{\mathbf{E}}]$ for the travelling wave dielectrophoretic force, neglecting the constants and the Clausisus-Mossotti factor. Simulations work with length ratios for the electrodes, not their real lengths. Force can be calculated from the simulation data by taking the particle size, Clausisus-Mossotti factor and electrode lengths into account.

Simulations are done for a parallel electrode configuration, as shown in Figure 4.1.

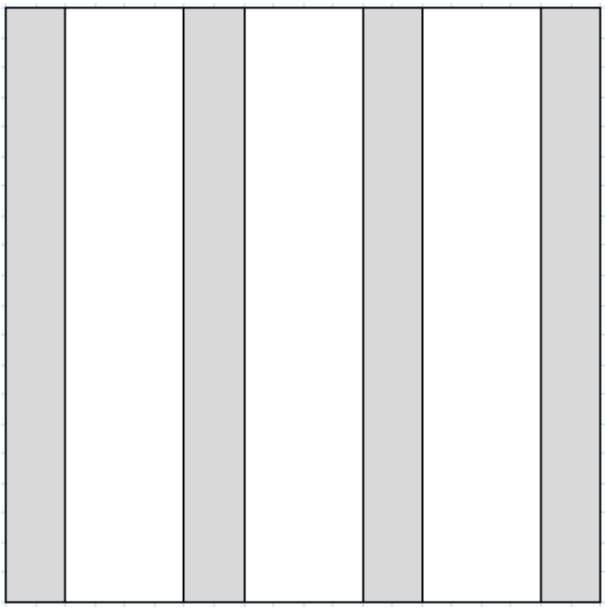

Figure 4.1: Parallel electrode array.

4.1 Analytical simulations

Analytical simulations are probably the most straightforward ones in terms of implementation. Simulations give the force at specific coordinates, given the electrode to gap ratio and the voltage. Figure 4.2 shows an example of an analytic solution. Analytic solution with approximate boundary condition is calculated using Equation (3.1). The simulation is calculated by function `anF2` (located in file `anF2.m`). Analytic solution with exact boundary condition is calculated using Equation (3.2) and is calculated by function `anF` (found in file `anF.m`).

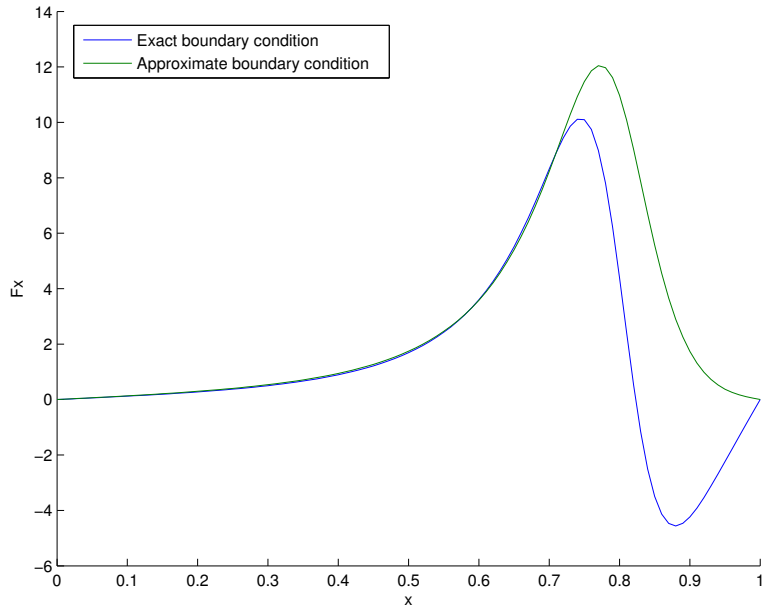

Figure 4.2: x-component of the force for analytic solution for $d_1/d_2 = 4$ electrode ratio, $V = 1$[V], $y = 0.1$. Units of length are dimeonsionless.

4.2 Numerical simulations

Simulations were done in 2D and in 3D using Comsol Multyphysics software. In creating FEM simulations it is important to correctly define the domain as well as boundary conditions.

4.2.1 2D

Simulations in 2D were based on [2]. The first simulation is of a parallel electrode array with 180 degree phase shift between electrodes, meaning that when there is V potential on an electrode, there is $-V$ potential on its neighbours. The simulation is done for a single electrode making use of the symmetry between the electrodes. The boundary conditions on the sides are Dirichlet, since the midpoint between V and $-V$ potentials is 0. Simulation can be found in file `DEPnum(1el).mph`. Figure 4.3 shows results of the simulation. Arrows indicate the direction of the force and the background colour is the logarithm of the force intensity, with maximum and minimum values adjusted for visibility purposes.

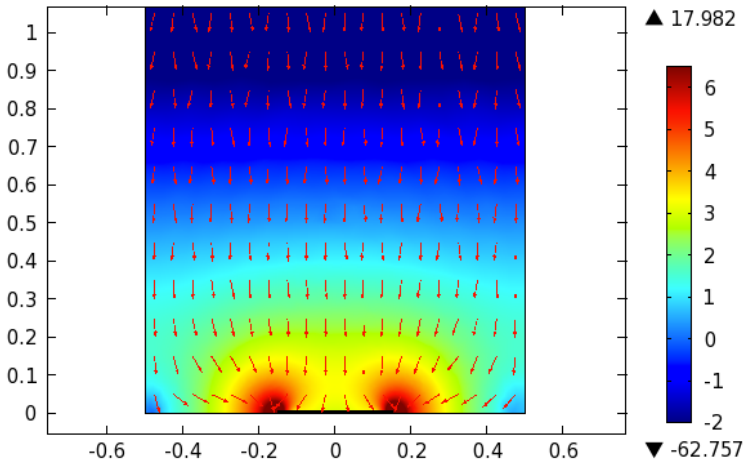

Figure 4.3: Numerical simulation: 180 ° phase shift. Side view. Electrode is in the middle.

Next numerical simulation is of a parallel electrode array with 90 degree phase shift between neighbouring electrodes. In this set-up travelling wave dielectrophoresis starts to show. Figures 4.4 and 4.5 show the results of the simulation. The simulation is done as described in section 3.2. Both Dirichlet and Neumann conditions are used. Simulation is in the file DEPnum.mph.

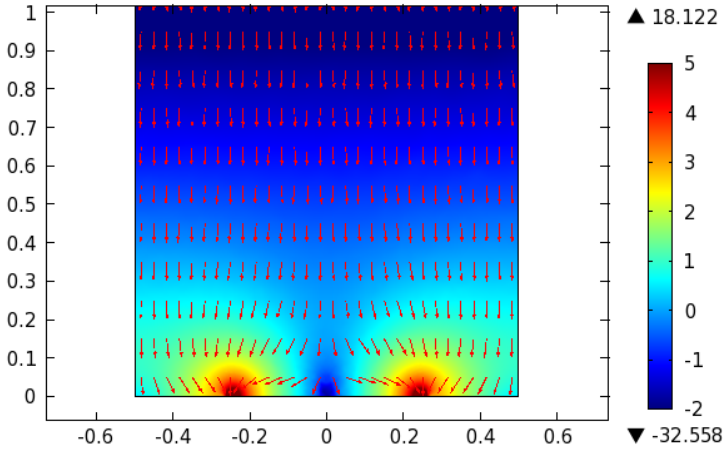

Figure 4.4: 2D Numerical simulation: 90 ° phase shift dielectrophoresis. Side view. Electrodes are on the sides, with a gap in the middle.

4.2.2 3D

Numerical simulations can also be used to create 3D models. Figure 4.6 shows a simulation of a 4 electrode parallel array. It shows the logarithmus of the dielectrophoretic force intensity in the zx-plane cutting through the middle of the electrodes. Care has to be taken with the boundary conditions. One way to deal with them is by placing them far enough from the area of interest so as to make their influence negligible. Simulation from Figure 4.6 is located in the file `DEPnum3d.mph`.

One disadvantage of 3D numerical simulations in Comsol is the speed. It takes a few minutes to calculate a simple 4 electrode array model as shown in

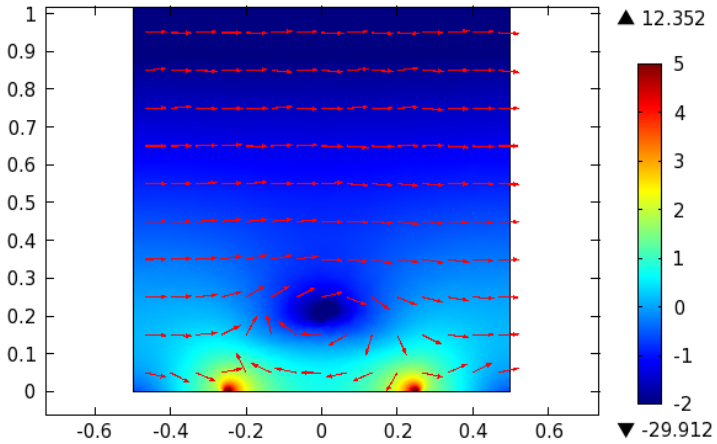

Figure 4.5: 2D Numerical simulation: 90° phase shift travelling wave dielectrophoresis. Side view. Electrodes are on the sides, with a gap in the middle.

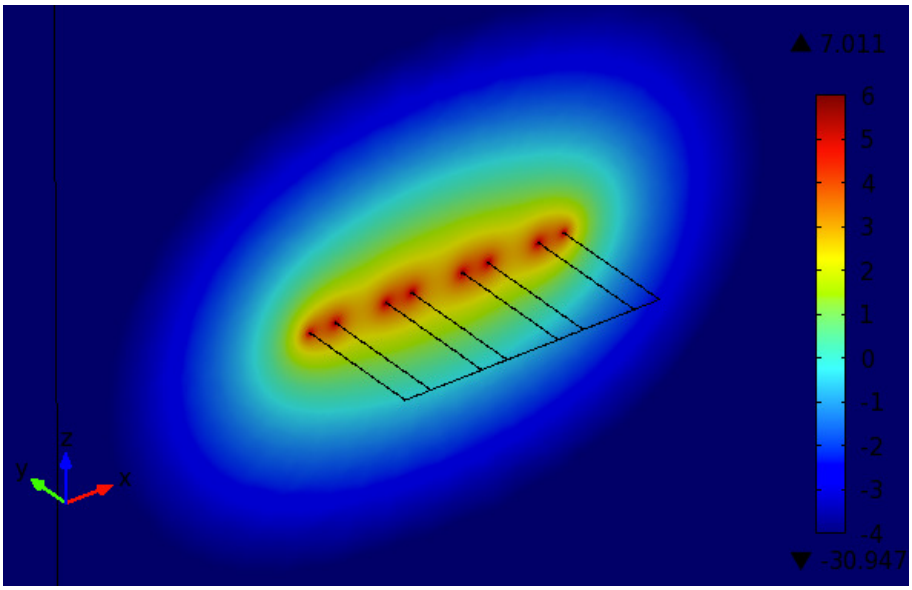

Figure 4.6: 3D Numerical simulation

Figure 4.6. This makes it infeasible to use for simulations of more complicated arrays, especially in real time.

4.3 Hybrid simulations

Hybrid simulations are the main subject of study in this report. They allow for much faster calculations than the numerical simulations, but take considerably more effort to implement. A lot of the problems arise at the Comsol-Matlab interface. In this section simulations will be presented alongside with unsuccessful attempts.

Hybrid simulation consists of two parts: preprocessing and force calculation. In the preprocessing stage the capacitance matrix for a specific electrode array is calculated which is then used to find the force given the potentials on individual electrodes. The capacitance matrix only needs to be calculated once for one electrode arrangement, it can then be stored and used when required.

In order to find the capacitance matrix, we have to be able to find the surface charge density. The process consists of applying 1 V potential to one electrode and 0 V to all the other ones, calculating the surface charge denstiy across all the electrodes and then approximating it as a matrix of single point charges. Approximation is done by dividing the electrode plane into a grid of smaller subareas. The surface charge density is then integrated over each subarea and the result assigned to a point charge which is in the middle of each subarea. For an n electrode array this process has to be repeated for $(n-1)$ electrodes.

4.3.1 Preprocessing - Comsol export

The first attempt at preprocessing was through the use of Comsol `'export data'` feature. The surface charge density was calculated directly in Comsol, then exported into a file using the `'export data'` feautre. The data was then

loaded in Matlab and interpolated using the `TriScatteredInterp` function. This did not work, as the data got damaged somewhere along the way and the output was meaningless.

4.3.2 Preprocessing - Live-Link, mphinterp

Second attempt was made by using Live-Link Matlab interface in Comsol. The data was requested using `mphinterp` function from Live-Link interface. It was then interpolated using `TriScatteredInterp` function. It was then integrated over subareas and the capacitance matrix was found. The approach worked well, however there were some numerical errors which arose during interpolation and integration.

4.3.3 Preprocessing - Live-Link, integration in Comsol

Third attempt used Live-Link, but requested Comsol for the integrated value for each subarea directly. This approach proved to give results with least numerical error, when compared against the data in Comsol, however it took very long time to process.

4.3.4 Preprocessing - splitting electrodes into subareas in Comsol

Fourth attempt involved splitting electrodes into subareas directly at the time of the model creation in Comsol. This did not work, because Comsol returned meaningless data when queried for the charges on the electrodes.

4.3.5 Preprocessing - Method of Moments

As an alternative, a preprocessing technique was thought of which would leave out Comsol altogether and calculate the surface charge density directly in Matlab. This was done using the Method of Moments technique, as described in section 3.5.2. The $\mathbf{P}$ matrix was calculated using two different approaches from two different sources[5, 1] which both gave near-identical ma-

trices. The result, however, varied from the Comsol result by a magnitude of 2 or more for different electrode configurations, while agreeing on the general shape of the charge distribution. An example of calculated charge density is shown in Figure 4.7. It shows a 4 parallell electrode array, with 1V potential on the first electrode and 0V potential on the other electrodes. The method of moments calculations are done in `surface_charge.m`. The electrode configuration can be defined in the form of an image file(e.g. `el4p2.png`).

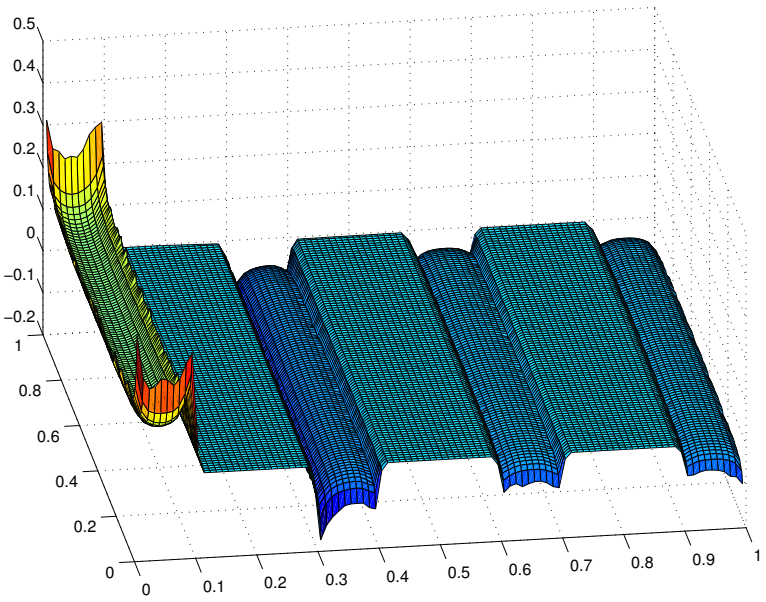

Figure 4.7: Surface Charge: MoM

4.3.6 Calculating the force

Equation (2.11) describes the dielectrophoretic force. We can see that in order to calculate it we need to know the constants: permittivitty of the medium, size of the particle and the Clausius-Mossotti factor for the given frequency and we need to know the square of the electric field. Electric

field can be calculated using Equation (3.3). Calculation of the force at an arbitrary point given the capacitance matrix and potentials on the electrodes is implemented in the function `forceAt`(in file `forceAt.m`). Calculation of force distribution in space is done in file `simulation.m`.

The force calculated in space over the electrodes is shown in Figure 4.8. The hybrid simulation takes considerably less time to calculate the force, once preprocessing is finished.

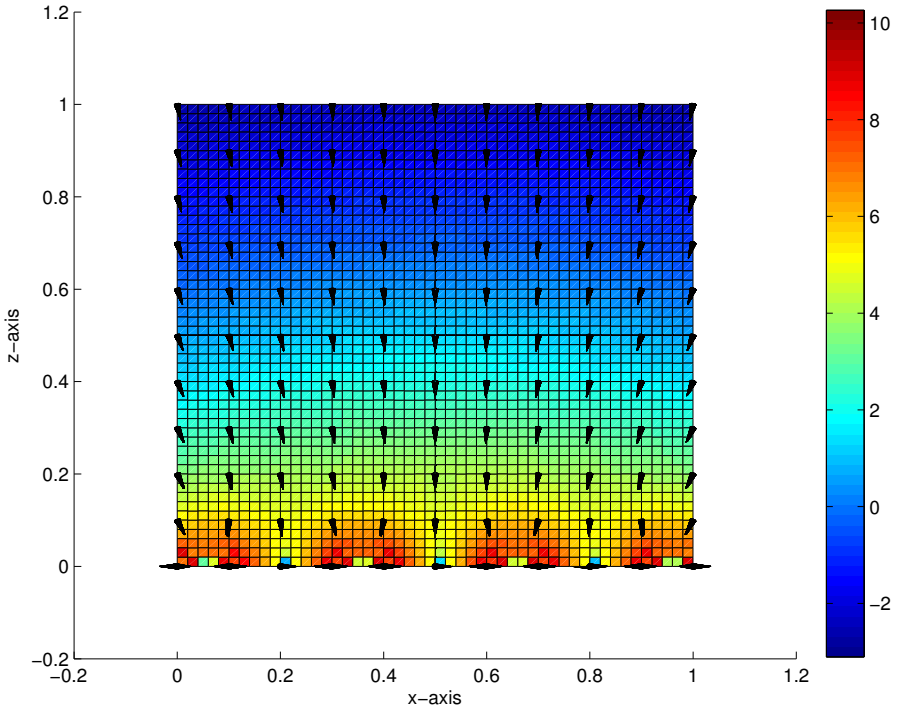

Figure 4.8: Hybrid 90° phase shift. View of the xz cut-plane. Arrows show the direction of the force, colour the intensity.

5 Results comparison

In this section the results of the simulations are compared with each other and then discussed. First we compare numerical results with analytical. Then hybrid vs. analytical. Then hybrid with the experimental resulsts.

Unfortunately, due to a Comsol error it was impossible to export data for analysis from a 3D numerical simulation.

5.1 Numerical vs. analytical

In this section we compare numerical results against analytical. The numerical results are exported from Comsol and then interpolated in Matlab. The analytical results are calculated directly in Matlab. The results are then plotted on a graph for visual comparison. Figures 5.1 and 5.2 show the comparison of the x and y components of the dielectrophoretic force. It can be seen that the numerical solution and the analytical solution with exact boundary conditions are very similar while the analytical solution with approximate boundary conditions differs for $x > 0.7$.

5.2 Hybrid vs. analytical

Here we compare hybrid results with analytical. The hybrid simulation is used for an array of 10 electrodes, whose capacitance matrix was calculated using method of moments. The results are compared for one electrode in the middle of the array. The simulation is done from the middle of the gap to the left of the electrode to the middle of the gap to the right of the electrode. It is then recalculated to scale of the analytic solution and plotted on a graph. 0 on the graph represent the middle of the electrode in the calculation. Figures 5.4 and 5.6 show comparison of the simulations of the forces in x and y direction(z direction for the hybrid, as it is in 3D).

It can be seen that although the simulations differ in magnitude, the trends in general shape are similar for both simulations. In case of the force

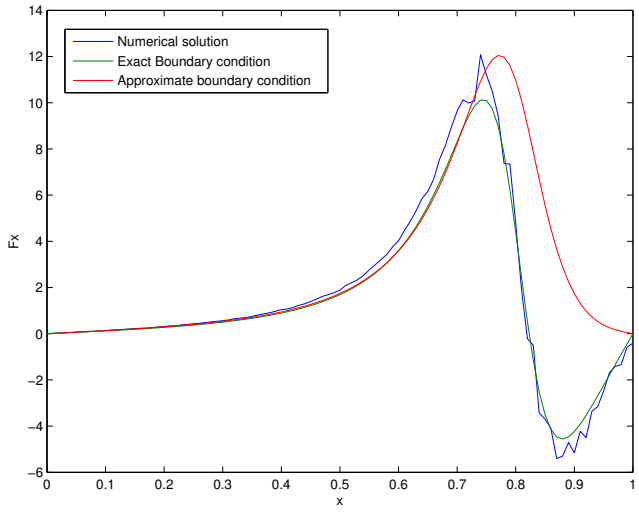

Figure 5.1: Comparison of numerical and analytical simulations. Force in x direction for electrode ratio $d_1/d_2 = 4$, $y = 0.1$.

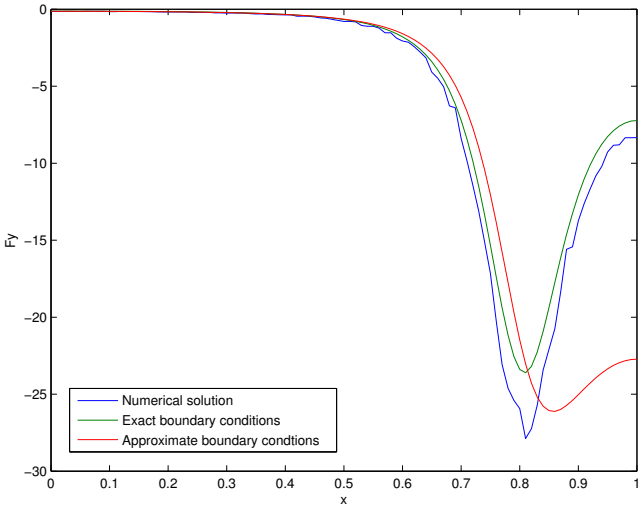

Figure 5.2: Comparison of numerical and analytical simulations. Force in y direction for electrode ratio $d_1/d_2 = 4$, $y = 0.1$

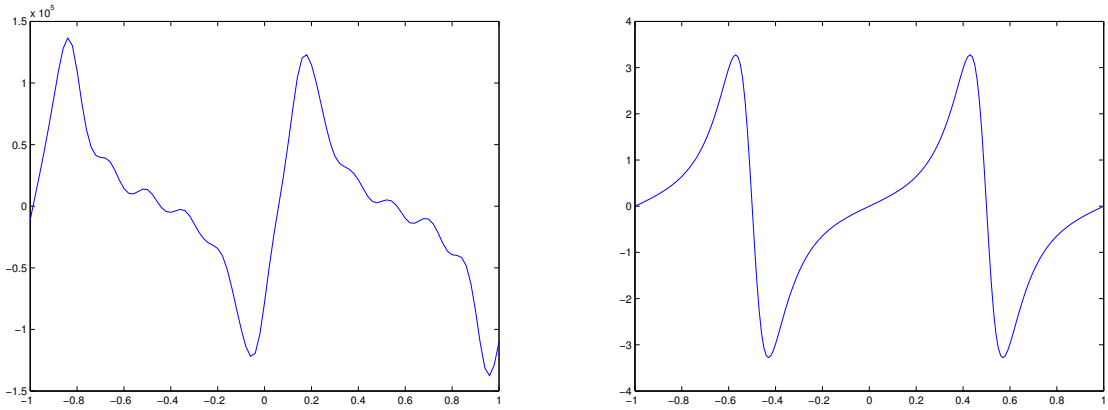

Figure 5.3: Force in x direction, hybrid simulation on the left, analytic on the right.

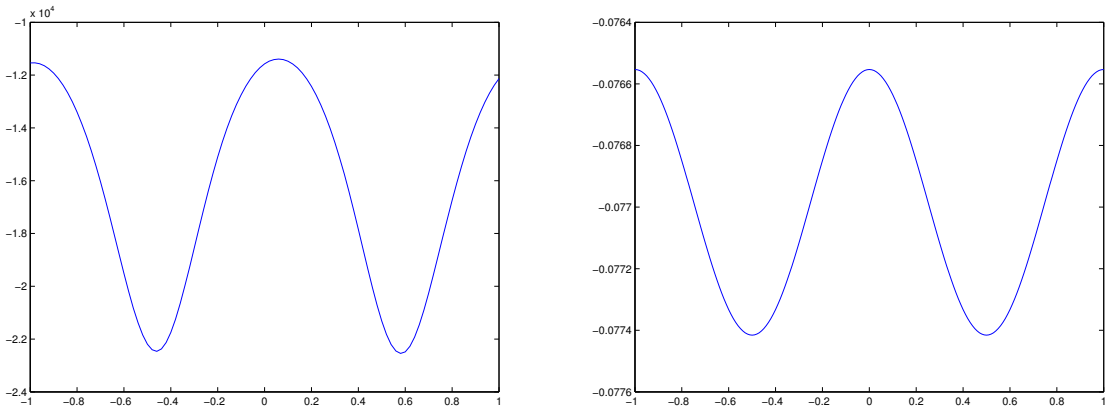

Figure 5.4: Force in x direction, hybrid simulation on the left, analytic on the right.

in x direction the force is always directed towards the edges of the electrodes. For the force in y direction the force varies in a very similar way for both simulations, increasing over the edges of the electrodes and decreasing over the gaps.

5.3 Hybrid vs. experimental

Experimental results were obtained for a parallel array of electrodes of width $100\,\mu$m and width to gap ratio 1:1. The particles were polystyrene, $50\,\mu$m in diameter. The applied voltage was $7\,V$ and the frequency was $400\,kHz$. The medium was deionised water. Only one electrode was activated at a time, while the rest remained at zero potential. A photo of the experiment is shown in Figure 5.5.

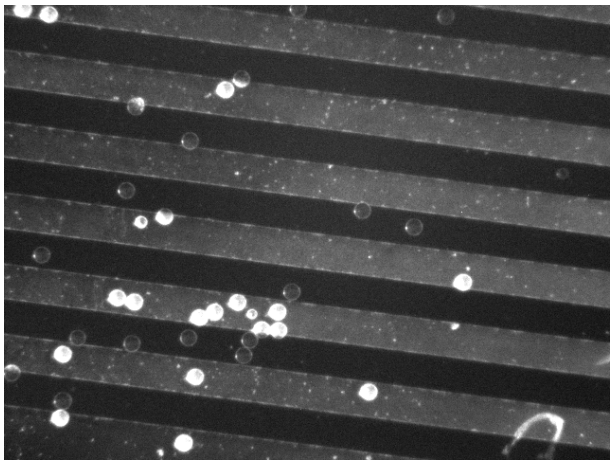

Figure 5.5: Photo of the experiment.

For the given frequency and materials the dielectrophoresis is negative. This is supported by the experiment in which the particle always moves away from the active electrode. Simulation predicts the same behaviour. In Figure 5.6 it can be seen that the force is in the direction away from the active electrode. In negative dielectrophoresis particles go in the direction

of decreasing gradient. Particle stops after a certain distance, because the absolute force diminishes significantly with distance.

Only some particles moved during the experiment, while the majority remained stationary. This can be attributed to weak Van der Waals forces that keep the particles attached to the electrodes or to the gaps between them.

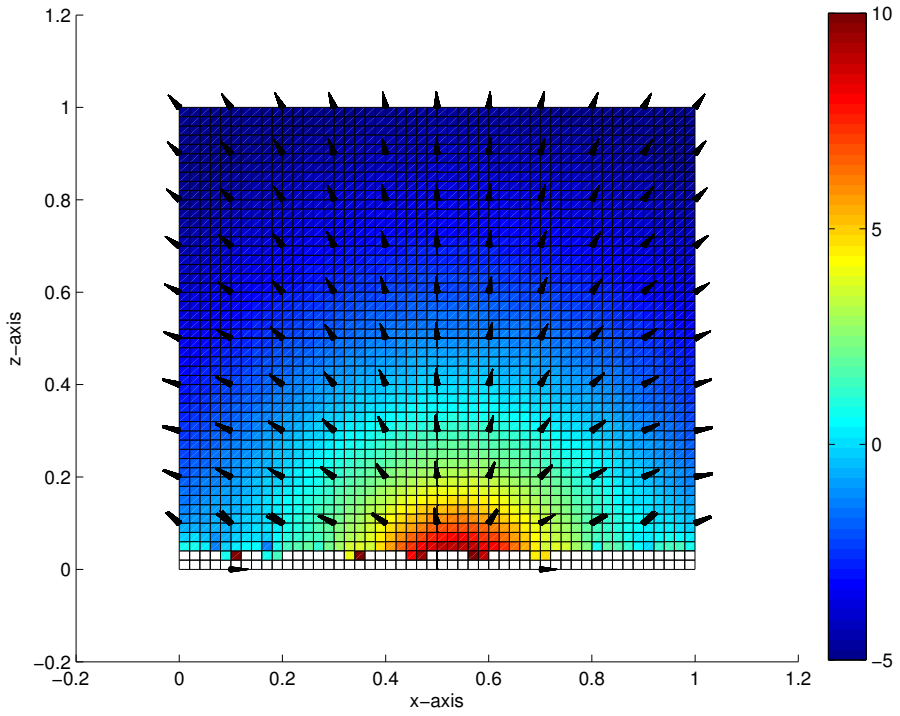

Figure 5.6: Simulation, negative dielectrophoresis. 6th electrode is active, the rest are at zero potential.

6 Conclusion

In this work we have looked at several ways of simulating dielectrophoretic forces. Analytical, numerical and hybrid simulations were implemented and compared against each other.

Hybrid simulation exhibited similar trends in the shape of the force direction over the electrode array, however there were significant differences in magnitude when compared with numerical and analytical simulations. This can be attributed to an error that the author was unable to identify. The experimental results agreed with the simulation predictions.

The simulation was implemented in a way that will allow it to work with more complex electrode arrays. It can potentially be used for designing a regulator.

In creating the simulation various books and scientific articles were consulted. The full list is provided below.

References

[1] Michael Pycraft Hughes. *Nanoelectromechanics in Engineering and Biology*. CRC Press, 2003.

[2] H. Morgan N.G. Green, A. Ramos. Numerical solution of the dielectrophoretic and travelling wave forces for interdigitated electrode arrays using the finite element method. *Journal of Electrostatics*, 56:235–254, 2002.

[3] Igor Mezic Dong Eui Chang, Sophie Loire. Closed-form solutions in the electrical field analysis for dielectrophoretic and travelling wave inter-digitated electrode arrays. *Journal of Physics D: Applied Physics*, 36:3073–3078, 2003.

[4] Nicolas Chaillet Mohamed Kharboutly, Michael Gauthier. Modeling the trajectory of a micro particle in a dielectrophoresis device. *Journal of Applied Physiscs*, 106, 2009.

[5] MF Iskander. Electromagnetics. Available at: http://tinyurl.com/momcharge.

Appendix - list of files

anF.m calculates the dielectrophoretic force using the analytical solution with exact boundary condition

anF2.m calculates the dielectrophoretic force using the analytical solution with approximate boundary condition

CMf.m calculates the Clausius-Mossotti factor

cmp.m plots graphs for different solutions

findC.m a function that interpolates and integrates data from Comsol, used in preprocess.m

forceAt.m function that returns the dielectrophoretic force at specific point in space given C matrix and the electrode potentials

genfield.m function used in surface_charge.m

im2el.m function that converts image to electrode data

Imm.m function that is used in surface_charge.m

PM.m function used in simulation.m and forceAt.m

preprocess.m calculates the C matrix using Comsol, works with Live-Link Comsol

Qf.m function used in simulation.m and forceAt.m

simulation.m calculates the force for a grid in space. plots the results

surface_charge.m calculates the C matrix using Method of Moments

DEPnum(1el).mph Comsol simulation

DEPnum(4ratio).mph Comsol simulation

DEPnum(tw).mph Comsol simulation

DEPnum3d.mph Comsol simulation

DEPnum4.mph Comsol simulation

C(4el)100(c2).mat C matrix for 4 electrode parallel array, calculated in Comsol, using 2nd method

C(el10)125(m).mat C matrix for 10 electrode parallel array, calculated in Matlab, using MoM method

C(el15)200(m).mat C matrix for 15 electrode parallel array, calculated in Matlab, using MoM method

***.png** images of electrodes, for use with surface_charge.m